JPE 17-5-10

https://doi.org/10.6113/JPE.2017.17.5.1223
ISSN(Print): 1598-2092 / ISSN(Online): 2093-4718

Torque Ripple Reduction of an Interior PM Synchronous Motor by Compensating Harmonic Currents Based on Flux Linkage Harmonics

Myung Joon Nam*, Jong Hyun Kim*, Kwan-Yuhl Cho†, Hag-Wone Kim*, and Younghoon Cho**

*,†Department of Control and Instrumentation Engineering, Korea University of Transportation, Chungju, Korea
**Department of Electrical Engineering, Konkuk University, Seoul, Korea

Abstract

The back emf harmonics of a permanent magnet (PM) synchronous motor is a major source of torque ripple. For torque control applications including column fitted MDPS (motor driven power steering) systems, it is essential to reduce the mechanical vibrations due to torque ripples at low speeds. In this paper, a torque ripple reduction algorithm for interior PM synchronous motors is proposed. The harmonic currents that cancel the 6th order torque harmonic are added to the nominal *dq* currents for MTPA (maximum torque per ampere) operation. The compensated harmonic currents are derived from flux linkage harmonics based on a FFT analysis of the back emf harmonics. Simulation and experimental results verify that the 6th order torque harmonic and THD of the torque ripple are reduced by compensating the *dq* harmonic currents.

Key words: Back emf harmonics, Flux linkage harmonics, MDPS, PMSM, Torque ripple

I. INTRODUCTION

For energy savings and the reduction of CO_2 emissions, electric vehicles and hybrid electric vehicles are an issue nowadays. In addition, some hydraulic controlled mechanical systems have been replaced by electric motor driven systems, such as power steering and brake systems. Compared with hydraulic power steering system, MDPS (motor driven power steering) has shown better fuel efficiency and better steering feeling in addition to being more environment friendly offering more space in the engine compartment due to the reduced components [1], [2]. In small and middle size vehicles, a column fitted type is normally used, where the electric motor is mounted on the steering column. In MDPS systems, the high torque capability, low torque pulsations, and energy efficiency are the key factors. Therefore, brushed DC motors have been replaced by PM synchronous motors.

In column fitted MDPS systems, very low mechanical vibrations are required since the motors of such systems are directly attached below the steering handle. Mechanical vibrations are mainly generated by the torque ripples of the PM synchronous motor so that reducing the torque ripples is essential, especially in the applications of torque control such as MDPS and in the main traction of electric vehicles. The sources of torque ripples in PM synchronous motors are the cogging torque, the offset of the current sensors, the resolution of the rotor position sensors, and the interaction of the back emf harmonics and the distorted current waveforms due to dead-time and back emf harmonics. Many techniques have been presented to reduce torque ripples [3]-[17], and they can be categorized into two approaches. These approaches are the motor structure approach and the motor control approach. The motor structure approach focuses on cogging torque reduction by the skewed rotor, the fractional slots, increasing the air-gap, adding notches in the surface of stator, and optimization of the stator teeth shape [3]-[5]. The motor control approach deals with sensors for detecting the current and rotor position, current waveforms, and back emf harmonics. The offset of the measured currents in the current sensors makes torque ripples with the fundamental frequency, which can be removed by current offset compensation and current sensor calibration [6]. In [7], an offset current compensation to reduce the phase currents distortion caused by switching device voltage drops and dead time is presented.

Manuscript received May 2, 2017; accepted Jun. 11, 2017
Recommended for publication by Associate Editor Kwang-Woon Lee.
†Corresponding Author: kycho@ut.ac.kr
Tel: +82-43-841-5329, Fax: +82-43-841-5320, Korea Nat'l Univ. of Transportation
*Department of Control & Instrumentation Engineering, Korea National University of Transportation, Korea
**Department of Electrical Engineering, Konkuk University, Korea

Even though the phase currents are sinusoidal and without distortion, torque ripple may be generated by the back emf harmonics.

The major source of torque ripples in PM synchronous motor is the mutual interaction between the back emf harmonics and the stator currents. To reduce the torque ripples due to back emf harmonics, the cancellation of selected torque harmonics with an extra harmonic current injection to the current reference has been suggested [8]-[17]. The dominant torque harmonics due to back emf harmonics are the 6th and 12th order components. As a result, a compensating current with the 6th and 12th harmonics is added to the current reference. Compensating harmonic currents can be derived from a nonlinear analysis of magnet saturation [8], and the measured torque ripples from torque sensors [9]. These methods have been applied to surface mounted PM synchronous motors using only *q*-axis current compensation, and they need to measure the torque ripples from torque sensors.

Various current control schemes based on direct torque control including repetitive control, predictive control and resonant control for torque ripple reduction have been presented [11]-[17]. The repetitive current control was presented to overcome the high frequency bandwidth of the current control to track the high frequency harmonic current reference for reducing the torque ripples due to back emf harmonics [11], [12]. The repetitive controllers require a more complex tuning process even though only the *q*-axis current is compensated in surface mounted PM synchronous motors. The predictive torque control with stator flux estimation [13], [14] can reduce the ripples of the torque and flux by selecting voltage vectors to reduce the cost function based on the prediction of the torque and stator flux in the next sampling instant. The torque and flux estimation is based on the fundamental components of the magnet flux. Therefore, the torque ripple due to the magnet flux harmonics cannot be reduced. The model predictive torque control [15] reduces the torque ripple by estimating the torque ripple due to back emf harmonics and cogging torque. However, the calculation of the cost function is complex and the relationships among the torque ripple, back emf harmonics and *dq* currents are not analyzed. The resonant controllers [16], [17] provide zero steady-state error at harmonic frequencies due to the infinite gain in their open-loops. In these resonant controllers, the frequency adaptation is not easy due to the requirement for variable sampling in variable speed drives. In addition, they considered only surface mounted PM synchronous motor. As a result, complicated modifications may be required for the case of an interior PM synchronous motor.

In this paper, torque ripple reduction for an interior PM synchronous motor by compensating harmonic currents based on the magnet flux harmonics is presented. The magnet flux harmonics are derived from a FFT analysis of back emf waveforms. The compensation *dq* currents that cancel the 6th order torque ripples are calculated from the nominal *dq* currents of MTPA operation and the magnet flux harmonics. Simulation and experimental results verify the effectiveness of the proposed algorithm.

II. Torque Ripple Reduction of IPMSM with Harmonic Currents Compensation

A. Modeling of a PMSM with Flux Linkage Harmonics

The voltage equation of a PM synchronous motor in the *abc* frame can be expressed as (1), where v_{abc} and i_{abc} are the stator voltages and stator currents, respectively, and r_s and L_s denote the phase resistances and phase inductances, respectively.

$$v_{abc} = r_s i_{abc} + \frac{d}{dt}\lambda_{abc} = r_s i_{abc} + \frac{d}{dt}(L_s i_{abc}) + \frac{d}{dt}\phi_{abcf} \tag{1}$$

λ_{abc} is the total stator flux linkages, which consist of the stator flux generated by the stator currents and the magnet flux of the rotor. The magnet flux, ϕ_{abcf}, has harmonic components due to a non-sinusoidal flux distribution and the harmonic components can be expressed by the magnitude and the phase difference to the fundamental component as given in (2).

$$\begin{aligned}\phi_{af} &= \sum_{k=1}^{\infty}\phi_{fk}\cos(k\theta_r + \alpha_k) \\ &= \phi_f\cos\theta_r + \phi_{f2}\cos(2\theta_r + \alpha_2) + \phi_{f3}\cos(3\theta_r + \alpha_3) + \cdots\end{aligned} \tag{2}$$

The back emf of the stator windings generated by the permanent magnet is the time derivative of the magnet flux. Therefore, the back emf of phase *a* can be expressed as (3).

$$\begin{aligned}e_{an} &= \frac{d}{dt}\phi_{af} = -\omega_r\sum_{k=1}^{\infty}k\cdot\phi_{fk}\sin(k\theta_r + \alpha_k) \\ &= -\omega_r\cdot(\phi_f\sin\theta_r + 2\phi_{f2}\sin(2\theta_r + \alpha_2) + 3\phi_{f3}\sin(3\theta_r + \alpha_3) + \cdots)\end{aligned} \tag{3}$$

Fig. 1 shows the phase and line to line back emf waveforms of a PM synchronous motor for a MDPS at 1,000rpm. The PM synchronous motor has 8 poles so that the period of one electrical cycle is 15msec at 1,000rpm. Fig. 2 shows a FFT analysis of the phase back emf. The dominant harmonic components are the 5th, 7th, and 11th harmonics, and the other harmonic components are small. Only the magnitude of the harmonic components is needed to derive the THD from the FFT analysis. However, the phase of the harmonic components when compared with the fundamental component as well as the magnitude of the harmonic components should be considered to analyze the torque ripple. The phase for the dominant harmonic components are marked as blue colored circles in Fig. 3(b). The phases of the 7th and the 11th harmonics are 0.3deg and 5.1deg, respectively. They are nearly in phase with the fundamental component. However, the 5th harmonic has a phase leading of 160.8deg. Measuring the magnet flux harmonics is difficult. However, they can be obtained from a FFT analysis of the back emf harmonics as shown in Fig. 2.

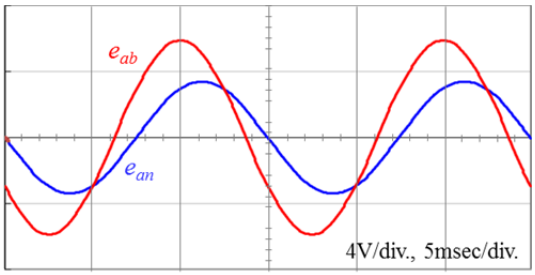

Fig. 1. Phase and line to line back emfs.

The voltage equation in the *abc* frame with the magnet flux harmonics of (1) can be transformed to the *dq* voltage equation in the rotor reference frame as (4).

$$\begin{aligned} v_d &= r_s i_d + \frac{d}{dt}\lambda_d - \omega_r \lambda_q \\ &= r_s i_d + L_d \frac{d}{dt} i_d - \omega_r L_q i_q - \omega_r \lambda_{qf\_har} \\ v_q &= r_s i_q + \frac{d}{dt}\lambda_q + \omega_r \lambda_d \\ &= r_s i_q + L_q \frac{d}{dt} i_q + \omega_r L_d i_d + \phi_f \omega_r + \omega_r \lambda_{df\_har} \end{aligned} \tag{4}$$

where λ_d and λ_q are the *d*-axis and *q*-axis total stator flux linkages, respectively. They can be expressed as (5) with *dq* flux linkage harmonics due to the magnet flux harmonics.

$$\begin{aligned} \lambda_d &= L_d i_d + \phi_f + \lambda_{df\_har} \\ \lambda_q &= L_q i_q + \lambda_{qf\_har} \end{aligned} \tag{5}$$

$$\begin{aligned} \lambda_{df\_har} &= \phi_{df\_har} + \frac{1}{\omega_r} \cdot \frac{d}{dt}\phi_{qf\_har} \\ &= -5\phi_{f5}\cos(6\theta_r + \alpha_5) + 7\phi_{f7}\cos(6\theta_r + \alpha_7) \\ &\quad -11\phi_{f11}\cos(12\theta_r + \alpha_{11}) + 13\phi_{f13}\cos(12\theta_r + \alpha_{13}) \\ \lambda_{qf\_har} &= \phi_{qf\_har} - \frac{1}{\omega_r} \cdot \frac{d}{dt}\phi_{df\_har} \\ &= 5\phi_{f5}\sin(6\theta_r + \alpha_5) + 7\phi_{f7}\sin(6\theta_r + \alpha_7) \\ &\quad +11\phi_{f11}\sin(12\theta_r + \alpha_{11}) + 13\phi_{f13}\sin(12\theta_r + \alpha_{13}) \end{aligned} \tag{6}$$

The torque of an interior PM synchronous motor including the flux linkage harmonics can be derived as (7). It is noted that the generated torque has both the 6th and 12th order torque harmonics caused by the flux linkage harmonics.

$$\begin{aligned} T_e &= \frac{3}{2} \cdot \frac{P}{2}(\lambda_d i_q - \lambda_q i_d) \\ &= \frac{3}{2} \cdot \frac{P}{2}\left((\phi_f + \lambda_{df\_har}) i_q - \lambda_{qf\_har} i_d\right) + \frac{3}{2} \cdot \frac{P}{2}(L_d - L_q) i_d i_q \end{aligned} \tag{7}$$

B. Compensated Currents for Canceling Torque Harmonics

The constant *dq* currents generate torque ripples by the interaction with the flux linkage harmonics as given in (7). In this paper, the compensating *dq* harmonic currents to reduce the selected torque harmonics are added to the nominal *dq* reference currents of the MTPA operation for a given reference torque. Let the *dq* reference currents consist of the nominal *dq* currents i_{dqo} and the compensating *dq* harmonic currents as (8), where i_{dh_har} and i_{qh_har} are the compensating

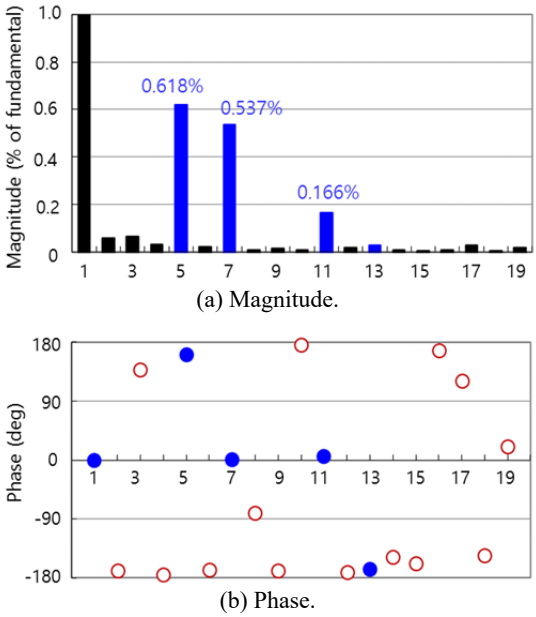

(a) Magnitude.

(b) Phase.

Fig. 2. FFT analysis of phase back emf.

d-axis and *q*-axis harmonic currents, respectively.

$$\begin{aligned} i_d &= i_{do} + i_{dh} \\ i_q &= i_{qo} + i_{qh} \end{aligned} \tag{8}$$

From (7) and (8), the magnetic torque can be expressed as (9), and the magnetic torque harmonics can be given as (10). In the magnetic torque harmonics, the product of the *dq* flux linkage harmonics and the *dq* harmonic currents are relatively small and can be neglected. Therefore, the compensating *q*-axis harmonic current can be derived as (11). The *q*-axis harmonic current that cancels the magnetic torque harmonics depends on the flux linkage harmonics and the *dq* nominal currents.

$$T_{mag} = \frac{3P}{4}\left((\phi_f + \lambda_{df\_har})(i_{qo} + i_{qh}) - \lambda_{qf\_har}(i_{do} + i_{dh})\right) \tag{9}$$

$$\begin{aligned} T_{mag\_har} &= \frac{3P}{4}\left(\phi_f i_{qh} + \lambda_{df\_har} i_{qo} + \lambda_{df\_har} i_{qh} - \lambda_{qf\_har} i_{do} - \lambda_{qf\_har} i_{dh}\right) \\ &\approx \frac{3P}{4}\left(\phi_f i_{qh} + \lambda_{df\_har} i_{qo} - \lambda_{qf\_har} i_{do}\right) = 0 \end{aligned} \tag{10}$$

$$i_{qh} = \frac{-\lambda_{df\_har} i_{qo} + \lambda_{qf\_har} i_{do}}{\phi_f} \tag{11}$$

The reluctance torque with *dq* harmonic currents can be given as (12) from (7) and (8). Similar to the magnetic torque harmonics cancellation, the reluctance torque harmonics can be given as (13) and the *d*-axis harmonic current can be derived as (14). The *d*-axis harmonic current that cancels the reluctance torque harmonics depends on the *dq* nominal currents and the *q*-axis harmonic current of (11).

$$T_{rel} = \frac{3P}{4}(L_d - L_q) i_d i_q = \frac{3P}{4}(L_d - L_q)(i_{do} + i_{dh})(i_{qo} + i_{qh}) \tag{12}$$

$$\begin{aligned} T_{rel\_har} &= \frac{3P}{4}(L_d - L_q)(i_{qo} i_{dh} + i_{do} i_{qh} + i_{dh} i_{qh}) \\ &\approx \frac{3P}{4}(L_d - L_q)(i_{qo} i_{dh} + i_{do} i_{qh}) = 0 \end{aligned} \tag{13}$$

TABLE I
PARAMETERS OF A PM SYNCHRONOUS MOTOR

Parameters	Value
Number of stator teeth	12
Number of poles (P)	8
Rated torque (T_e)	5.1Nm
Phase resistance (r_s)	14.0 mΩ
d-axis inductance (L_d)	52.0 uH
q-axis inductance (L_q)	59.0 uH
Back emf constant (ϕ_f)	8.036 mVsec

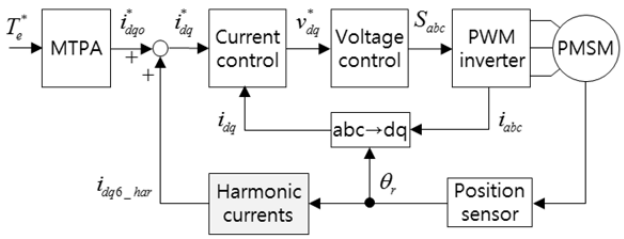

Fig. 3. Torque control of PMSM with harmonic currents compensation.

$$i_{dh} = -\frac{i_{do}}{i_{qo}} \cdot i_{qh} \tag{14}$$

III. SIMULATION AND EXPERIMENTAL RESULTS

The interior PM synchronous motor used in this paper has 12 stator teeth and 8 poles in the rotor as shown in Table I. The rated current is 85Arms for a rated torque of 5.1Nm, and the stator resistances and back emf constant are very small since a 12V battery is used as the DC link capacitor.

Fig. 3 shows a block diagram of the proposed torque ripple reduction algorithm. The torque reference generates the dq nominal reference currents for MTPA operation. The compensating dq harmonic currents come from the dq flux linkage harmonics of (6), (11), and (14). The dq reference currents consist of the dq nominal currents and dq harmonic currents that cancel the torque ripples caused by the flux linkage harmonics. In MDPS applications, mechanical vibration is serious at low speeds. Therefore, the test is performed at 60rpm. The electrical frequency for the 6th and 12th order harmonic currents are 24Hz and 48Hz, respectively. The bandwidth of the PI current controller in this type of application is commonly 300Hz ~ 400Hz for the stability of the current controller. Therefore, the 12th harmonic currents have a phase delay to the reference currents. In addition, the 6th order torque harmonic is relatively larger than the 12th torque harmonic. As a result, only the 6th order harmonic currents are compensated with the reference currents.

Fig. 4 shows the dq flux linkage harmonics at 60rpm derived from the measured back emf harmonics. The d-axis nominal flux linkage is 8.036mWb. In addition, the 6th order harmonic is dominant and its magnitude is 0.093mWb. On the other hand, the average of the q-axis nominal flux linkage is zero and it includes the 12th order harmonics.

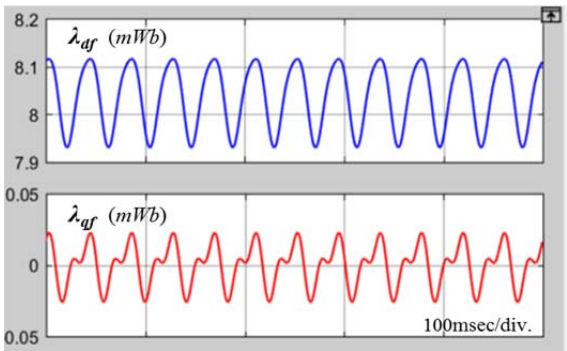

Fig. 4. dq flux linkages due to permanent magnet.

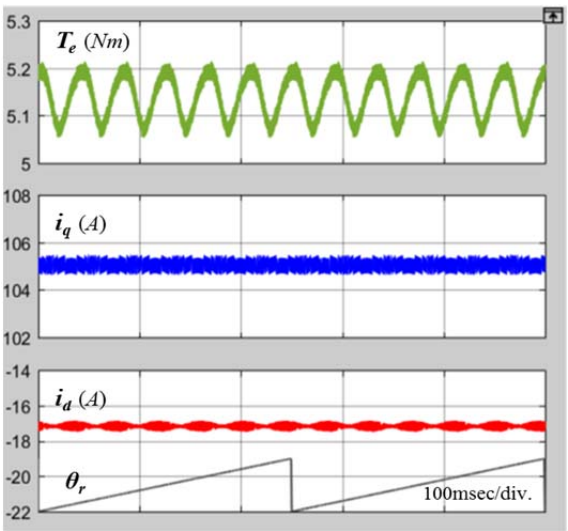

Fig. 5. Simulation results of torque and dq currents of conventional control at 60rpm.

Fig. 5 shows simulation results of the torque ripple and dq currents of the conventional control at 60rpm. The nominal dq currents are -17A and 105A for MTPA operation at a 5.1Nm load, respectively. The peak to peak value of the torque ripple is 0.12Nm, which is 2.4% of the rated load. In addition, the phase of the torque ripple is almost coincided with $\cos\theta_r$. The torque harmonic components obtained by a FFT analysis are shown in Fig. 6. The 6th and 12th order harmonics are 1.16% and 0.17%, respectively. The 6th order harmonic is dominant, and the THD of the torque harmonics to the average torque is 1.21%.

Fig. 7 shows the dq harmonic reference currents to reduce the 6th order torque harmonic. The dq harmonic reference currents are derived from (11) and (14), and the amplitude of the q-axis harmonic reference current is 1.2A. Fig. 8 shows simulation results of the torque ripple and dq currents of the proposed control with harmonic currents compensation at 60rpm. A FFT analysis of the torque ripple is shown in Fig. 9. The dq current is the sum of the nominal dq reference currents and the dq harmonic currents to cancel the 6th order torque harmonic. As shown in Fig. 8 and Fig. 9, the 6th order

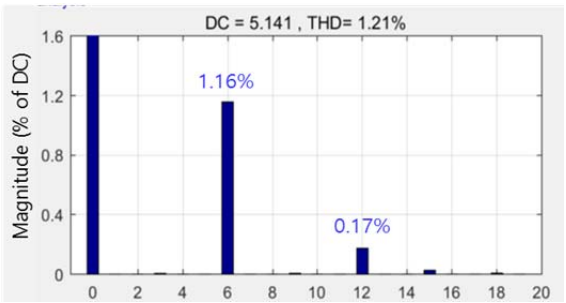

Fig. 6. FFT analysis of the torque ripples of the conventional control.

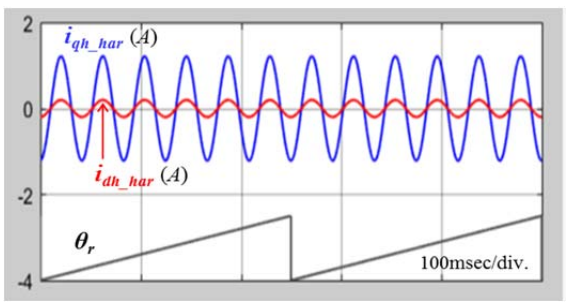

Fig. 7. Compensating *dq* harmonic reference currents.

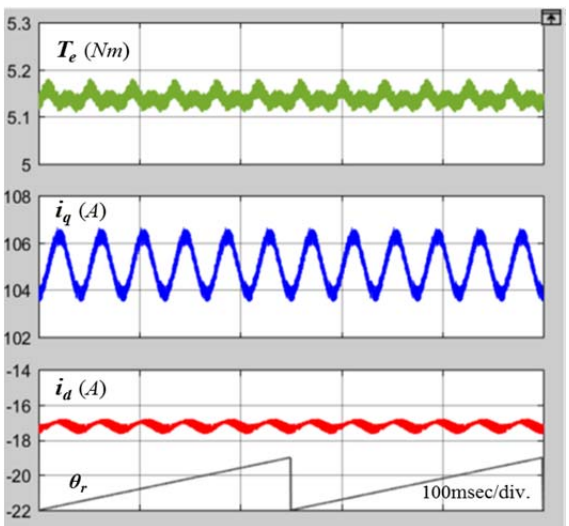

Fig. 8. Simulation results of the torque and *dq* currents of the proposed control at 60rpm.

torque harmonic is reduced to 0.18% from the 1.18% of the conventional control by compensating the *dq* harmonic currents. The THD of the torque ripple to the average torque is also reduced to 0.39% from 1.21%. The 12th order torque harmonic is not reduced since the 12th order harmonic reference current is not compensated.

Fig. 10 shows the experimental setup of the dynamo set. The torque ripple reduction algorithm is implemented by a TMS320F28335. The current control frequency is 10kHz and the bandwidth of the current control is 300Hz. Fig. 11 shows experimental results of the *dq* currents and torque ripple of the conventional control at 60rpm. The torque harmonic components by a FFT analysis are also shown in Fig. 12. The

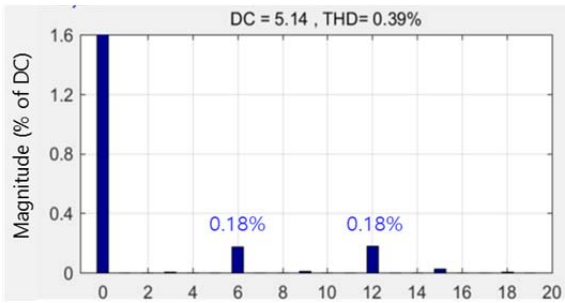

Fig. 9. FFT analysis of the torque ripples of the proposed control.

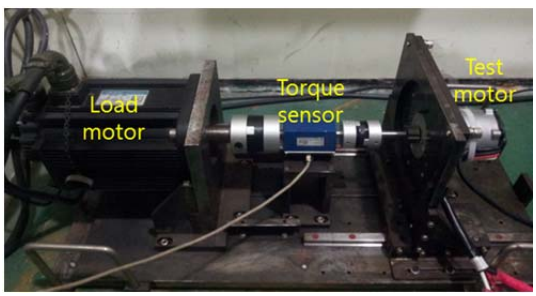

Fig. 10. Experimental setup.

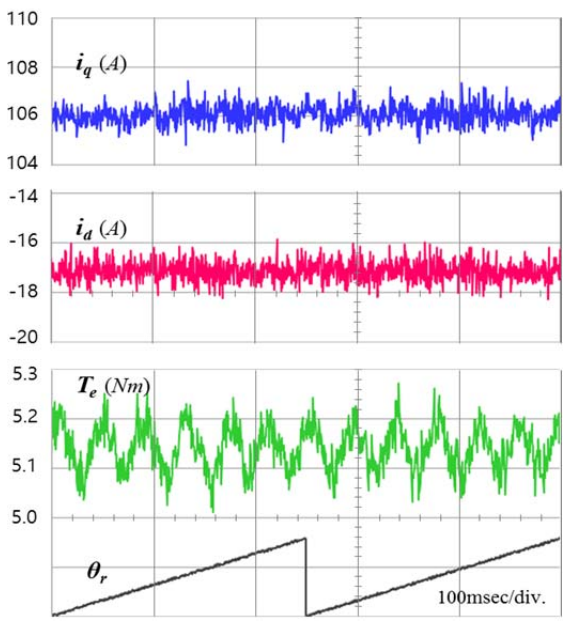

Fig. 11. Experimental results of the torque and *dq* currents of the conventional control at 60rpm.

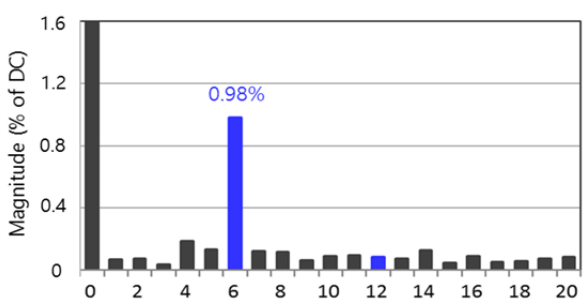

Fig. 12. FFT analysis of the torque ripples of the conventional control at 60rpm.

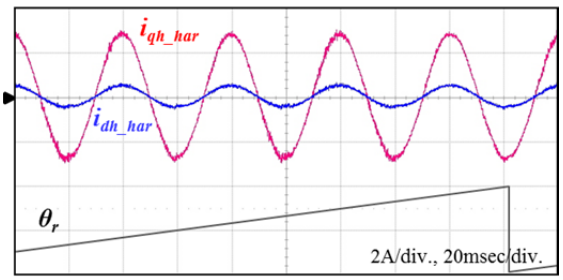

Fig. 13. Compensating the *dq* harmonic reference currents.

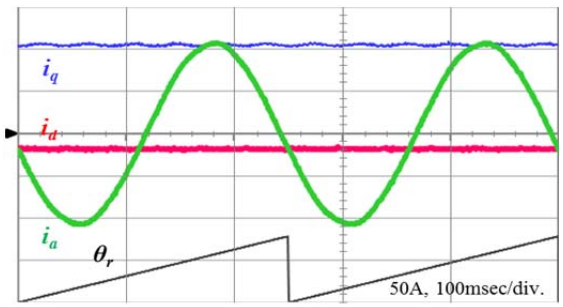

Fig. 14. *dq* currents and phase *a* current at 60rpm.

nominal *dq* currents are -17A and 106A for MTPA operation at a 5.1Nm load, respectively. The peak to peak value of the torque ripple is 0.17Nm, which is 3.3% of the rated load. The 6th order harmonic is 0.98%, the other harmonic components are lower than 0.2%, and the THD of the torque ripple is 1.07%.

Fig. 13 shows the *dq* harmonic reference currents to reduce the 6th order torque harmonic, where the amplitude of the *dq* harmonic reference currents are 0.25A and 1.3A, respectively. Fig. 14 shows the *dq* currents and phase current. The average *dq* currents are -17A and 106A, respectively, and the lead angle of the phase current for MTPA operation is 9.0deg.

Fig. 15 shows the experimental results of the *dq* currents and torque ripple of the proposed control at 60rpm, while the torque harmonic components are shown in Fig. 16. The 6th order torque harmonic is reduced to 0.32% from 0.98% and the THD of the torque ripple is also reduced to 0.45% from 1.07%. Compared with the conventional control, it can be seen that the 6th order torque harmonic and THD are significantly reduced by compensating the *dq* harmonic currents.

Fig. 17 shows the torque ripples of the conventional control and proposed control at 30rpm, while similar waveforms at 90rpm are shown in Fig. 18. Fig. 19 shows the 6th order torque harmonics for the conventional and proposed control at 30rpm, 60rpm, and 90rpm. As shown in Fig. 19, the 6th order torque harmonics are reduced at 30rpm and 60rpm by the harmonic currents compensation. The reduction of the 6th order torque harmonics at 90rpm is not effective enough since the harmonic currents are not fully compensated by the limit on the bandwidth of the current controller. It is noted that the torque harmonics at 90rpm can be reduced by increasing the bandwidth of the current controller if the stability of the current control is guaranteed.

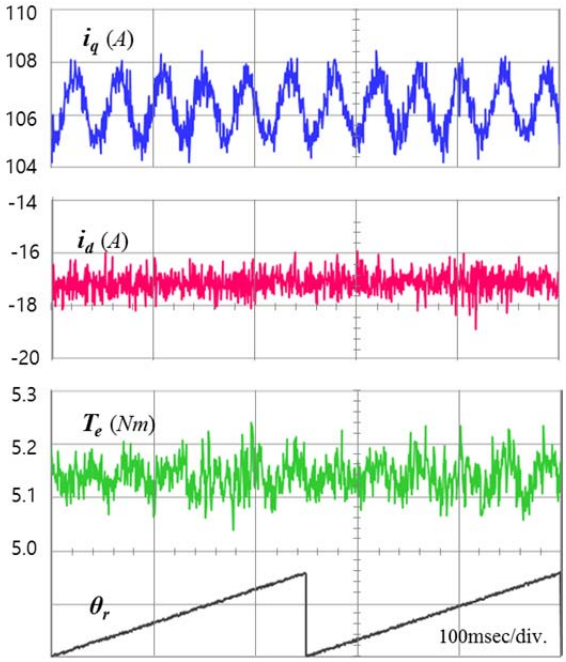

Fig. 15. Experimental results of the torque and *dq* currents of the proposed control at 60rpm.

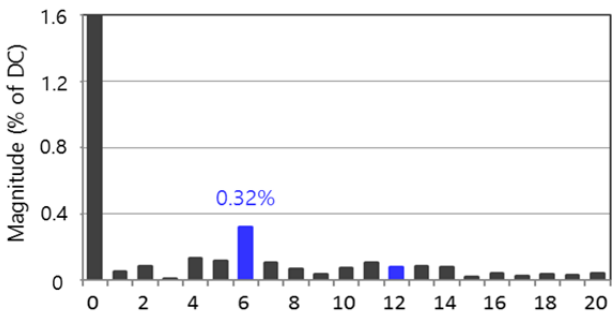

Fig. 16. FFT of torque ripple of proposed control at 60rpm.

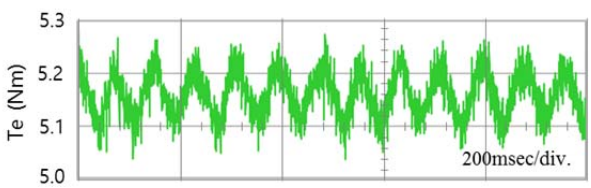

(a) Conventional control.

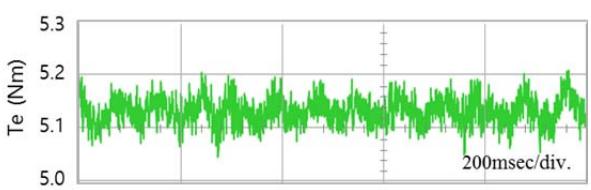

(b) Proposed control.

Fig. 17. Torque ripples at 30rpm.

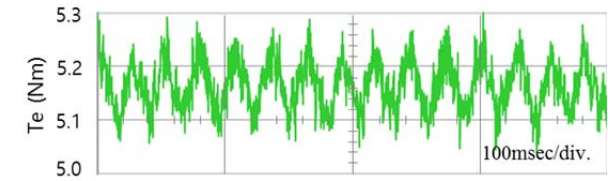

(a) Conventional control.

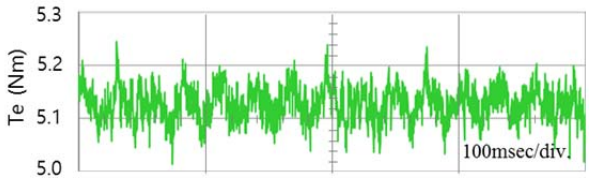

(b) Proposed control.

Fig. 18. Torque ripples at 90rpm.

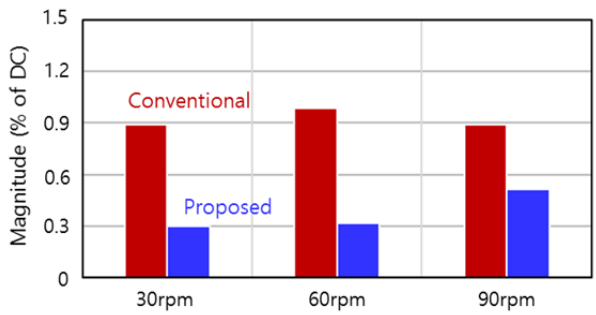

Fig. 19. 6th order torque harmonics for conventional and proposed control.

IV. Conclusions

In this paper, a torque ripple reduction algorithm for the interior PM synchronous motors used in MDPS is proposed. To reduce the torque ripples caused by the flux linkage harmonics of the permanent magnet, the 6th order harmonic currents are added to the nominal *dq* currents. The compensating *dq* harmonic currents are derived from the *dq* flux linkage harmonics based on a back emf harmonics analysis. It is verified though simulation and experimental results that the 6th order torque harmonic and THD of the torque ripple at low speeds are significantly reduced by compensating harmonic currents.

Acknowledgment

This work was supported by "Human Resources Program in Energy Technology" of the Korea Institute of Energy Technology Evaluation and Planning (KETEP), granted financial resource from the Ministry of Trade, Industry & Energy, Republic of Korea. (No. 20164030201100)

References

[1] A. W. Burton, "Innovation drivers for electric power assisted steering," *IEEE Contr. Syst. Mag.*, pp. 30-39, Nov. 2003.

[2] H. Eki, T. Teratani, and T. Iwasaki, "Power consumption and conversion of EPS systems," in *Power Conversion Conference (PCC)*, pp. 1333-1339, 2007.

[3] K. Y. Cho, H. W. Kim, and Y. H. Cho, "Review of BLAC motor and drive technology for electric power steering of vehicles, *Journal of the Korea Academia-Industrial Cooperation Society*, Vol. 12, No. 9, pp. 4083-4094, Sep. 2011.

[4] Y. Sim, N. Niguchi, and K. Hirata, "A novel asymmetrical half-type IPM bldc motor structure for reducing torque ripple," *Transactions of Korean Institute of Power Electronics (KIPE)*, Vol. 21, No. 2, pp. 134-143, Apr. 2016.

[5] Y. K. Kim, S. H. Rhyu, and I. S. Jung, "Shape optimization for reduction the cogging torque of BLAC motor for EPS application," in *International Conference on Electrical Machines and Systems (ICEMS)*, 2010.

[6] H. Tamura, T. Ajima, and Y. Noto, "A torque ripple reduction method by current sensor offset error compensation," in *European Conference on Power Electronics and Applications (EPE)*, pp. 1-10, 2013.

[7] G. H. Lee, G. Y. Nam, J. Y. Lee, J. P. Hong, C. M. Lee, and G. S. Choi, "Reduction of torque ripple in AC motor drives for electric power steering," in *International Conference on Electric Machines and Drives (IEMDC)*, pp. 2006-2011, 2005.

[8] K. Y. Cho, Y. K. Lee, H. S. Mok, H. W. Kim, B. H. Jun, and Y. H. Cho, "Torque ripple reduction of a PM synchronous motor for electric power steering using a low resolution position sensor," *Journal of Power Electronics*, Vol. 10, No. 6, pp. 709-716, Nov. 2010.

[9] G. H. Lee, "Active cancellation of PMSM torque ripple caused by magnetic saturation for EPS applications," *Journal of Power Electronics*, Vol. 10, No. 2, pp. 176-180, Mar. 2010.

[10] M. J. Nam, J. H. Kim, K. Y. Cho, and H. W. Kim, "Torque ripple reduction of an interior PM synchronous motor for electronic power steering," in *International Conference of Power Electronics (ICPE)*, pp. 21-30, June 2015.

[11] P. Mattavelli, L. Tubiana, and M. Zigliotto, "Torque ripple reduction in PM synchronous motor drives using repetitive current control," *IEEE Trans. Power Electron.*, Vol. 20, No. 6, pp. 1423-1431, Nov. 2005.

[12] M. Tang, A. Gaeta, A. Formentini, and P. Zanchetta, "A variable frequency angle-based repetitive control for torque ripple reduction in PMSMs," in *International Conference on Power Electronics, Machines, and Drives (PEMD)*, pp. 1-6, 2016.

[13] M. Siami, D. A. Khaburi, and J. Rodriguez, "Torque ripple reduction of predictive torque control for PMSM drives with parameter mismatch," *IEEE Trans. Power Electron.*, Vol. 32, No. 9, pp. 7160-7168, Sep. 2017.

[14] H. Zhu, X. Xiao, and Y. Li, "Torque ripple reduction of torque predictive control scheme for permanent-magnet synchronous motors," *IEEE Trans. Ind. Electron.*, Vol. 59, No. 2, pp. 871-877, Feb. 2012.

[15] A. Mora, A. Orellana, J. Juliet, and R. Cardenas, "Model predictive torque control for torque ripple compensation in variable-speed PMSMs," *IEEE Trans. Ind. Electron.*, Vol.

63, No. 7, pp. 4584-4592, Jul. 2016.

[16] A. G. Yepes, F. D. Freijedo, P. F. Comesana, J. Malvar, O. Lopez, and J. D. Gandoy, "Torque ripple minimization in surface-mounted PM drives by means of PI + multi-resonant controller in synchronous reference frame," in *36th Annual Conference on Industrial Electronics Society (IECON)*, pp. 1017-1022, 2010.

[17] M. F. Iacchetti, G. D. Marquez, and R. Perini, "Torque ripple reduction in a DFIG-DC system by resonant current controllers," *IEEE Trans. Power Electron.*, Vol. 30, No. 8, pp. 4244-4254, Aug. 2015.

Myung Joon Nam received his B.S. and M.S. degrees in Control and Instrumentation Engineering from the Korea National University of Transportation, Chungju, Korea, in 2014 and 2016, respectively. Since 2016, he has been with VCTech, Korea. His current research interests include variable speed motor drives and power converters. He is a member of the Korean Institute of Power Electronics (KIPE).

Jong Hyun Kim received his B.S. and M.S. degrees in Control and Instrumentation Engineering from the Korea National University of Transportation, Chungju, Korea, in 2013 and 2015, respectively. Since 2015, he has been with Green Power, Korea. His current research interests include variable speed motor drives and power converters. He is a member of the Korean Institute of Power Electronics (KIPE).

Kwan-Yuhl Cho received his B.S. degree in Electrical Engineering from Seoul National University, Seoul, Korea, in 1986; and his M.S. and Ph.D. degrees in Electrical and Electronics Engineering from the Korea Advanced Institute of Science and Technology (KAIST), Daejeon, Korea, in 1988 and 1993, respectively. From 1993 to 2004, He worked at LG Electronics, Digital Appliance Research Lab., Seoul, Korea. Since 2004, he has been with the Department of Control and Instrumentation Engineering at the Korea National University of Transportation, Chungju, Korea. His current research interests include variable speed motor drives and power converters.

Hag-Wone Kim received his B.S. degree in Electrical Engineering from Korea University, Seoul, Korea, in 1989; and his M.S. and Ph.D. degrees in Electrical and Electronics Engineering from the Korea Advanced Institute of Science and Technology (KAIST), Daejeon, Korea, in 1991 and 2004, respectively. From 1991 to 2008, he worked at LG Electronics, Digital Appliance Research Lab., Seoul, Korea. Since 2008, he has been with the Department of Control and Instrumentation Engineering at the Korea National University of Transportation, Chungju, Korea. His current research interests include variable speed motor drives and power converters. He is the Editor in Chief in the Korean Institute of Power Electronics (KIPE) and a member of the Institute of Electrical and Electronics Engineers (IEEE).

Younghoon Cho was born in Seoul, Korea, in 1980. He received his Ph.D. degree in Electrical Engineering from the Virginia Polytechnic Institute and State University, Blacksburg, VA, USA. From 2004 to 2009, he was an Assistant Research Engineer at the Hyundai MOBIS R&D Center, Yongin, Korea. He is presently working as an Associate Professor in the Department of Electrical Engineering, Konkuk University, Seoul, Korea. His current research interests include power electronic circuits and control in vehicle and grid applications.